

A simple function for calculating the interaction between a molecule and a graphene sheet

Xiongce Zhao*

*Joint Institute for Computational Sciences and Center for Nanophase Materials Sciences,
Oak Ridge National Laboratory, Oak Ridge, Tennessee 37831, USA* †

We present a novel potential model for calculating the interaction between a molecule and a single graphene sheet. The dispersion/repulsion, induction, dipole-quadrupole, quadrupole-quadrupole interactions between a fluid molecule and a graphene sheet are described by integrated functions that are only dependent on the separation between the molecule and the graphene along its planar normal. The derived potential functions are in excellent agreement with the computationally demanding atom-explicit summation method. Typical errors of the integrated potential are less than 2% in the energy minimum compared with the exact atom-explicit summation. To examine the practical effectiveness of the newly developed functions, Monte Carlo simulations were performed to model the adsorption of two representative gases in graphene sheets using both the integrated and atom-explicit potentials. The integrated potential results in same adsorption isotherms and density profiles for the adsorbed phase while it only requires negligible computing time compared with that using the atom-explicit method. The newly developed potential functions provide a simple and accurate approach to calculating the physical interaction between molecules and graphene sheets.

I. INTRODUCTION

Graphene, or individual layers of graphite in which each carbon atom is bonded to three other carbon atoms, has been the subject of considerable research interest recently [1]. Being a representative two dimensional crystal, graphene has many peculiar properties such as low dimensionality, surface homogeneity, structure stability, conductivity, and charge transport ability. It is deemed as one of the most promising materials for future applications in various fields such as electronics, novel materials, sensors, biodevices etc. [1–13].

In the investigations of fundamental properties of graphene, it is often of great interest to understand the interaction of molecules with graphene on a molecule level. For example, graphene sheets have been used as high-sensitivity sensors [8] or background membranes [14] in studying the behavior of individual molecules. In such applications, interaction between the target molecule and the graphene is one of the key properties that needs to be understood in order to design effective devices. Therefore, a simple and reliable approach to estimating the graphene-fluid interaction is essential. Furthermore, computer simulation, which is becoming a useful partner of experiments in studying fluid-solid interactions, requires realistic and computationally affordable method with sufficient accuracy to calculate the molecule-solid interactions, such as that between molecules and graphene sheets. However, to our knowledge, a simple and accurate function describing the interaction between a molecule and a single graphene sheet is still not available. In this paper, we attempt to develop a novel potential to solve

this problem.

There are two general approaches to calculating the interactions between a molecule and a crystal solid like graphene. One can use an atom-explicit potential to describe the interaction between each atom in the molecule and each atom in crystal, calculating the total potential energy by summing up all pairs of atoms. Dispersion, repulsion, electrostatic and induction interactions can all be computed in this way. But such an approach is computationally costly, especially for large systems involving significant number of solid atoms. Alternatively, one can develop integrated potential functions that accounts for all the solid atoms in an effective way, making use of the periodicity and homogeneity in the distribution of atoms in the crystal. This has been a popular and useful approach for modeling solid-fluid interactions for many systems, including graphite and metals [15]. Integrated potentials are easy to program and very efficient computationally.

In this paper the second approach was employed to derive a new set of effective potential force fields for molecules on a graphene sheet. The types of solid-fluid interactions of interest include the dispersion and repulsive (Lennard-Jones, or LJ), the induction due to the dipole in the molecule and the polarizability of carbon atoms in graphene, and the interaction between multipoles in the molecule and the permanent quadrupole in graphene. The potential functions derived in this work are extensions of a previous work by us [16] for modeling interaction between gases and a semi infinite graphitic surface. The accuracy of the derived potentials are evaluated by comparing the energies calculated from the integrated expressions and those from atomistic summation approach. The effectiveness of the potentials are demonstrated by using the derived formulas in simulating the adsorption of two representative gases into slits composed of single graphene sheets.

In Section II, the functions are derived. Section III

*Electronic address: xiongce.zhao@nih.gov

†Current address: NIDDK, National Institutes of Health, Bethesda, MD 20892, USA

and IV are examinations of the new potentials via comparison with atomistic summation methods. Section V is concluding remarks.

II. POTENTIAL DEVELOPMENT

We assume that a molecule is located right above the center of a single graphene sheet. The origin of the system was set as the mass center of the molecule. If we only consider the pairwise interactions, the total potential energy between the molecule and the graphene can be expressed by a summation

$$U = \sum_i^{\infty} u(r_i), \quad (1)$$

where $r_i = (x_i, y_i, z)$ denotes the position of a carbon atom in graphene relative to the molecule, $u(r_i)$ is the pairwise potential between the molecule and carbon atom i in graphene, which is only dependent on the separation between them, $r_i = (x_i^2 + y_i^2 + z^2)^{1/2}$. For a graphene sheet of infinite size along its lateral directions (x and y), U only depends on the separation between the molecule and graphene along its surface normal z , and Eq.(1) becomes

$$U(z) = \sum_i^{\infty} u(x_i, y_i, z). \quad (2)$$

For example, the Lennard-Jones interaction between the molecule and a carbon atom is given as

$$u(r) = 4\varepsilon_{\text{sf}} \left[\left(\frac{\sigma_{\text{sf}}}{r} \right)^{12} - \left(\frac{\sigma_{\text{sf}}}{r} \right)^6 \right], \quad (3)$$

where ε_{sf} and σ_{sf} are the LJ potential parameters for the cross interaction between the molecule and a graphene carbon atom. Substituting Eq.(3) into Eq.(2) gives

$$U(z) = \sum_i^{\infty} 4\varepsilon_{\text{sf}} \left[\frac{\sigma_{\text{sf}}^{12}}{(x_i^2 + y_i^2 + z^2)^6} - \frac{\sigma_{\text{sf}}^6}{(x_i^2 + y_i^2 + z^2)^3} \right], \quad (4)$$

If we assume that the graphene sheet is homogeneous and continuous along its x and y directions, $U(z)$ can be approximated by an integral over x and y

$$U(z) = 4\varepsilon_{\text{sf}} d_s \int_0^{\infty} \int_0^{\infty} \left[\frac{\sigma_{\text{sf}}^{12}}{(x^2 + y^2 + z^2)^6} - \frac{\sigma_{\text{sf}}^6}{(x^2 + y^2 + z^2)^3} \right] dx dy, \quad (5)$$

where d_s is the density of carbon atoms in a unit graphene area $dx dy$. The integration can be simplified by letting $x^2 + y^2 = S$, which gives $dx dy = \pi dS$. Then Eq.(5) reduces to

$$U(z) = 4\pi\varepsilon_{\text{sf}} d_s \int_0^{\infty} \left[\frac{\sigma_{\text{sf}}^{12}}{(S + z^2)^6} - \frac{\sigma_{\text{sf}}^6}{(S + z^2)^3} \right] dS. \quad (6)$$

Eq.(6) leads to an integrated potential for the LJ interaction between a molecule and an infinitely large graphene sheet

$$U_{\text{LJ}}(z) = 2\pi\varepsilon_{\text{sf}}\sigma_{\text{sf}}^2 d_s \left[\frac{2}{5} \left(\frac{\sigma_{\text{sf}}}{z} \right)^{10} - \left(\frac{\sigma_{\text{sf}}}{z} \right)^4 \right]. \quad (7)$$

The derived expression Eq.(7) for the LJ interaction between a molecule and a graphene is analogous to a potential by Steele [15]. The interaction is only a function of the distance of the molecule from the graphene along its planar normal, z , thus the numerical calculation is substantially simplified. It is noteworthy to point out that unlike the potential for graphite [15] the new function for graphene, Eq.(7), does not contain any empirical term that requires fitted parameters. This is due to the fact that no approximation was involved in the derivation to account for the semi-infinite layers of graphene for a graphite surface. Only assumption here is that the atoms in graphene sheet are continuous, otherwise the derivation is strictly exact.

For LJ particles, Eq. (7) should be a sufficient approximation for calculating the molecule-graphene potential. However, for molecules that has partial charges or permanent multipole moments, additional polar interactions have to be included. For this purpose, similar procedures are applied to derive integrated forms for the induction and multipolar interactions between the molecule and a graphene sheet. We note that the above derivation procedure is applicable as long as the pairwise potentials are dependent only of r by an inverse power r^{-n} with $n > 1$. This condition is satisfied if we use point or angle-averaged dipoles and point quadrupoles for the molecule-graphene interaction. For example, the angle-averaged dipole-induced dipole interaction between a polar molecule and a carbon atom in the graphene is given by [17]

$$u_{\mu}(r) = -\frac{\mu_f^2 \alpha_s}{(4\pi\varepsilon_0)^2 r^6}, \quad (8)$$

where μ_f is the permanent dipole moment of the molecule, α_s is the isotropic polarizability of a carbon atom in graphene, and ε_0 is the vacuum permittivity.

The angle-averaged dipole-quadrupole interaction is given by [17]

$$u_{\mu\Theta}(r) = -\frac{\mu_f^2 \Theta_s^2}{kT(4\pi\varepsilon_0)^2 r^8}, \quad (9)$$

where Θ_s is the permanent quadrupole moment on each carbon atom in graphene, k is Boltzmann's constant and T is the absolute temperature.

Finally, the angle-averaged quadrupole-quadrupole interaction for the molecule and carbon atom is given by [17]

$$u_{\Theta\Theta}(r) = -\frac{14\Theta_f^2 \Theta_s^2}{5kT(4\pi\varepsilon_0)^2 r^{10}}, \quad (10)$$

TABLE I: The Lennard-Jones and multipole parameters for the example molecules studied.

	ϵ_f (kcal/mol)	σ_f (Å)	μ_f (Debye)	Θ_f (10^{-20} C Å ²)
CH ₄	0.2378	3.527	–	–
H ₂ O	0.1554	3.152	2.351	–
Cl ₂	0.7101	4.115	–	10.79

where Θ_f is the permanent quadrupole moment of the molecule.

Substituting Eqs. (8)–(10) into Eq.(2) and integrating, we obtain the following expressions. The integrated induction potential is

$$U_\mu(z) = -\frac{\pi d_s \mu_f^2 \alpha_s}{2(4\pi\epsilon_0)^2} \frac{1}{z^4}. \quad (11)$$

The integrated dipole-quadrupole potential is

$$U_{\mu\Theta}(z) = -\frac{\pi d_s \mu_f^2 \Theta_s^2}{3kT(4\pi\epsilon_0)^2} \frac{1}{z^6}. \quad (12)$$

The integrated quadrupole-quadrupole potential is

$$U_{\Theta\Theta}(z) = -\frac{7\pi d_s \Theta_f^2 \Theta_s^2}{10kT(4\pi\epsilon_0)^2} \frac{1}{z^8}. \quad (13)$$

Likewise, the potential functions in Eq.(11)–(13) are only dependent on the separation between the multipole and graphene along its planar normal z . By using Eq.(7) and Eqs.(11)–(13), one can calculate the interaction potential energy between a polar molecule and a graphene sheet without using the costly pairwise atomistic summation.

III. COMPARISON WITH ATOMISTIC POTENTIALS

To examine the accuracy of the derived functions, we calculated the potential energies of several representative nonpolar and polar molecules interacting with a single graphene sheet using the integrated functions Eqs.(7) and (11)–(13), to compare with those from atomistic summation of potentials Eqs. (3) and (8)–(10). The graphene sheet in the atomistic summation was modeled as a square about 10 nm in a side, containing 3680 carbon atoms. Trial calculations indicate that such a system size contains more than enough carbon atoms to approximate a graphene sheet that is infinite along its lateral directions. A single molecule was placed over the center of the graphene sheet and its interaction potential energies were computed by summing up interactions from each carbon atom.

The LJ and multipole potential parameters for the example molecules chosen are shown in Table I. The nonpolar molecule studied is methane, modeled by a single LJ

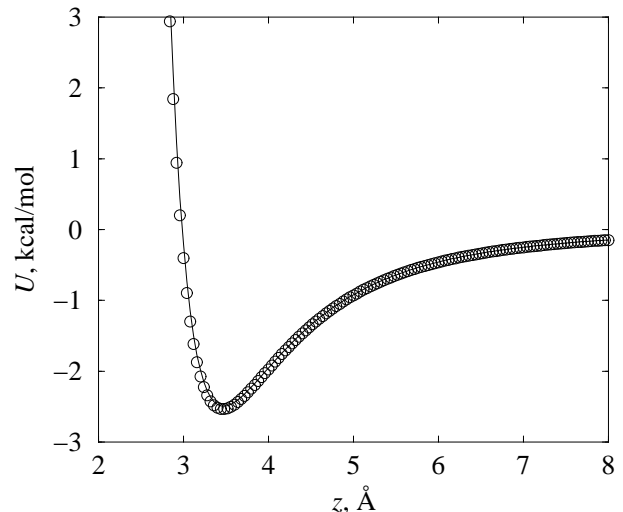


FIG. 1: Interaction of methane with a single graphene sheet calculated using the atom-explicit pairwise summation of Eq.(3) (line) and the integrated function Eq.(7) (symbols).

site [18]. The representative polar molecules selected are water and chlorine. Water is modeled by the SPC/E potential [19], with a strong dipole moment of 2.351 Debye. Please note that the LJ parameters of water in Table I are for the O atom. The chlorine molecule is modeled by a single LJ site plus a quadrupole moment of 10.79×10^{-20} C Å² [20]. The purpose of the calculation was to study the accuracy of the integrated potential compared with atomistic summation. Therefore, the potential models for the molecules were selected arbitrarily. The values of potential parameters for carbon atoms in graphene are $\sigma_s=3.40$ Å, $\epsilon_s=0.05569$ kcal/mol, $d_s=0.382$ Å⁻² [16], $\alpha_c=1.76$ Å³ [21], $\Theta_s=-3.03 \times 10^{-20}$ C Å² [22]. The cross interaction parameters ϵ_{sf} and σ_{sf} were calculated using the Lorentz-Bertholet rules.

In Figs. 1 to 3 we compare the potential energies calculated from the integrated potentials and the atom-explicit potentials at 300 K, for CH₄, H₂O, and Cl₂. It is seen that the integrated expressions are in excellent agreement with the atomistic summation results. If we take the atomistic summation results as the standard, the typical errors in the integrated potential are less than 2% at the energy minimum. The integrated functions always give a slightly more attractive potential compared to the atom-explicit methods, possibly due to the fact that we treat the graphene carbon atoms as continuum in the integrated potential.

The integrated potentials are most accurate when the graphene sheet is infinitely large. However, we also carried out series of calculations using graphene sheets of various sizes, to test the applicability of the derived functions to the finite-size graphene. We found that the integrated potentials are in excellent agreement with the atomistic potentials as long as the square-shaped graphene sheet contains more than ~ 500 carbon atoms

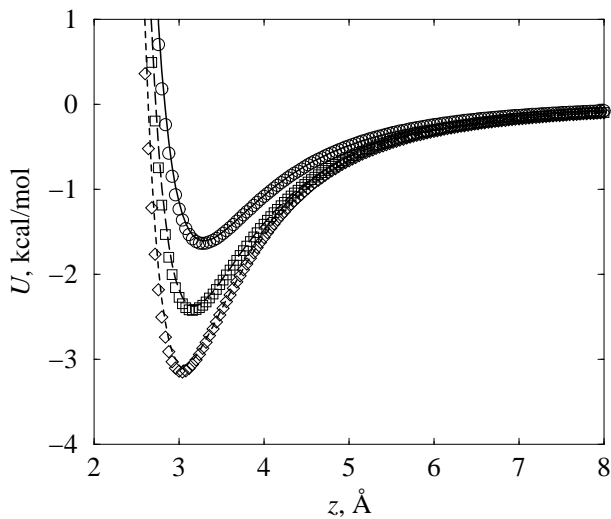


FIG. 2: Interaction of a water molecule with a single graphene sheet calculated using the atomistic summation (lines) and integrated functions (symbols). Atomistic summations: LJ interaction Eq.(3) (solid line), LJ plus induction interactions Eq.(3)+Eq.(8) (long dashed line), and LJ plus induction plus dipole-quadrupole interactions Eq.(3)+Eq.(8)+Eq.(9) (dashed line). Integrated functions: LJ interaction Eq.(7) (circle), LJ plus induction interactions Eq.(7)+Eq.(11) (square), and LJ plus induction plus dipole-quadrupole interactions Eq.(7)+Eq.(11)+Eq.(12) (diamond).

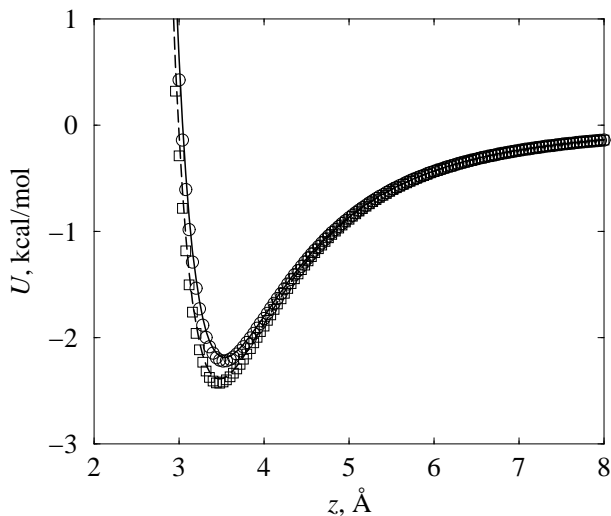


FIG. 3: Interaction of a chlorine molecule with a single graphene sheet calculated using the atomistic summation (lines) and integrated functions (symbols). Atomistic summations: LJ interaction Eq.(3) (solid line), LJ plus quadrupole-quadrupole interactions Eq.(3)+Eq.(10) (long dashed line). Integrated functions: LJ interaction Eq.(7) (circle), LJ plus quadrupole-quadrupole interactions Eq.(7)+Eq.(13) (square).

(or a graphene sheet of $\sim 38 \times 38 \text{ \AA}^2$). This suggests that the derived potentials can also be readily used in estimating the interaction of molecules with finite graphene sheets that are nanometer-scale in size.

For the different types of interactions between a molecule and graphene, it is interesting to see that, for example from Fig. 2, the induction and dipole-quadrupole interactions for strongly polar molecules such as water are non-negligible compared with the LJ energy. On the other hand, based on the Cl_2 example, the quadrupole-quadrupole interaction is usually not significant, even for molecules with a strong quadrupole moment like chlorine.

IV. APPLICATIONS IN ADSORPTION SIMULATION

One of important applications of the potential functions developed in this work is molecular simulation of adsorption of molecules in pores composed of single graphene sheets. In turn, such simulations serve as a verification of the accuracy and effectiveness of the integrated functions in practical applications. For this purpose, we chose to simulate the adsorption of two typical nonpolar and polar gases, methane and water, confined in single graphene sheets. The simulations were performed using the grand canonical Monte Carlo (GCMC) method, the detailed description of which can be found in literature [23].

The potentials parameters describing the interactions of water and methane with graphene are given in Table I. The methane is modeled as a simple one-site LJ particle, with a cutoff of 9 \AA . The LJ interaction between water molecules is also modeled by a cutoff of 9 \AA , without long-range correction applied, as suggested by the original literature [19]. The electrostatic interaction between water molecules are modeled by the partial charges distributed on the three charge sites on the water model, without long range correction. The interaction between the molecules and graphenes is calculated by either the atomistic summation approach or integrated functions for comparison.

The GCMC cell for adsorption simulations is a rectangular box. Two graphene sheets are placed in the cell with their planes parallel to the $x - y$ plane of the box. The distance between the two graphene layers along the z direction is 15 \AA . Again, this separation is chosen arbitrarily. Periodic boundary conditions are applied in all three directions. Therefore, the height of simulation box in the z direction is 30 \AA . The typical box sizes in the x and y directions are set as 32 and 34 \AA respectively, leading to a cell volume of about 33 nm^3 . The types of move attempted during a GCMC simulation were selected randomly with probability of 0.40 , 0.40 , 0.10 , and 0.10 for displacements, rotations, creations, and deletions of a fluid molecule respectively. For simulation of the spherical methane, the rotation moves were merged to displacement moves. Each simulation included equilibra-

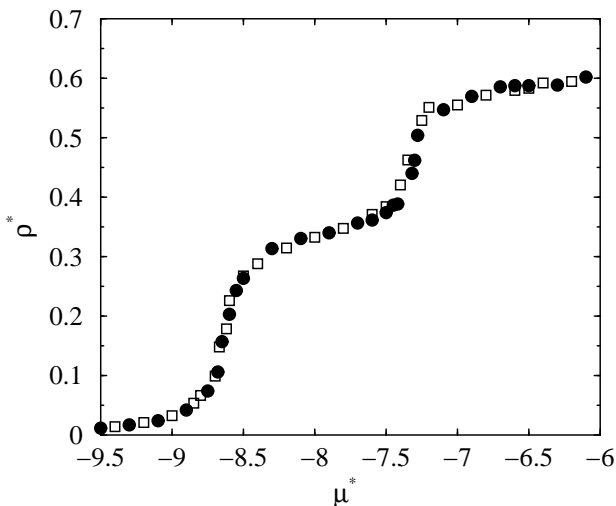


FIG. 4: Adsorption isotherm of methane in singlet graphene sheets at 77 K. Circles were calculated using the atomistic summation potential and squares were calculated using the integrated potential. Adsorbed amount (ρ^*) and chemical potential (μ^*) are in reduced unit.

tion of 2×10^6 MC moves and production of 2×10^6 MC moves.

The simulation of methane adsorption in graphene sheets were performed at 77 K [18]. Previous theoretical studies predict that water only wets graphitic carbon surfaces when temperature is above ~ 510 K [24, 25]. Therefore, we chose to perform simulations of water/graphene at 550 K. In GCMC simulations the reduced chemical potential was varied to obtain isotherms and density profiles of adsorbed methane or water, using either atomistic or integrated potential for comparison.

Calculated adsorption isotherms for methane in graphene sheets at 77 K are presented in Fig. 4. The circles are simulation results computed from the atomistic summation of Eq.(3), while the squares are from simulations using the integrated potential Eq.(7). It can be seen that, within statistical uncertainty, the isotherms from these two different potentials are in excellent agreement. The first plateau in the isotherm corresponds to the first layers of methane adsorbed on graphene sheets, and the second plateau is from the methane adsorbed onto first layers as chemical potential increases. This is confirmed by density profile distribution of the adsorbed phase shown in Fig. 5. The transition from nonadsorption to the first layer occurs at about $\mu^* = -8.6$, and the transition from the first to the second layer occurs at about $\mu^* = -7.3$.

It is known that the isotherm shapes, especially the layering transition of adsorbed phase calculated from simulations, are very sensitive to the solid-fluid interactions [26]. A small deviation in the solid-fluid potential can result in significant shift in the layer transition location in isotherms. The excellent agreement in the adsorption layering transition for the two potentials indicates

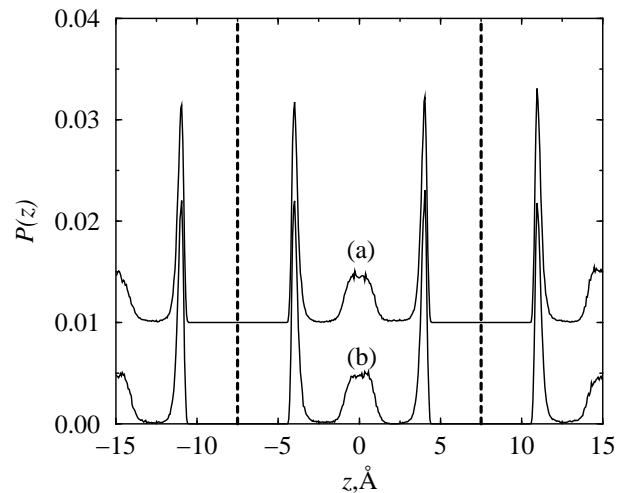


FIG. 5: Density profiles of methane adsorption in graphene sheets at 77 K and reduced chemical potential of -6.5 . (a) was calculated using the atomistic summation potential and (b) was calculated using the integrated potential. Two curves are almost identical so (a) was shifted by 0.01 in $P(z)$ for clarity. The dashed lines at $z = \pm 7.5$ \AA represent the two graphene sheets in the system.

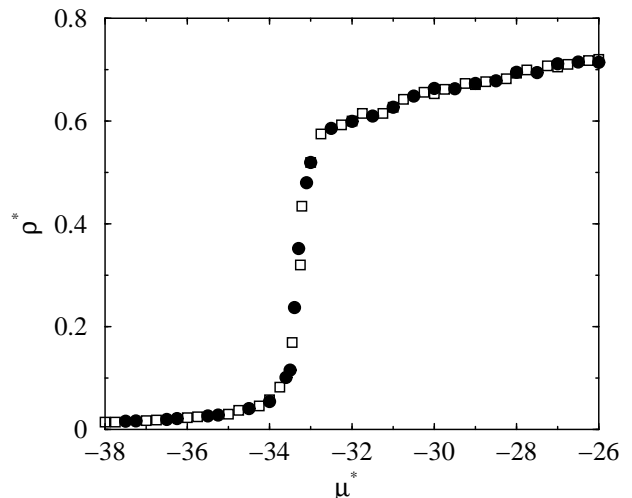


FIG. 6: Adsorption isotherm of water in graphene sheets at 550 K. Circles were calculated using the atomistic summation potential and squares were calculated using the integrated potential. Adsorbed amount (ρ^*) and chemical potential (μ^*) are in reduced unit.

that the integrated functions are robust alternatives to the atomistic models.

One example of density profiles of methane adsorbed in graphene layers is given in Fig. 5. Sharp peaks are observed at $z = \pm 4, \pm 11$ \AA , which correspond to the first adsorbed methane layers on the graphene sheets. Additional broad peaks are observed at $z = 0, \pm 15$ \AA , representing the adsorbed second layers between the first layers. Again, it is seen that the density distribution

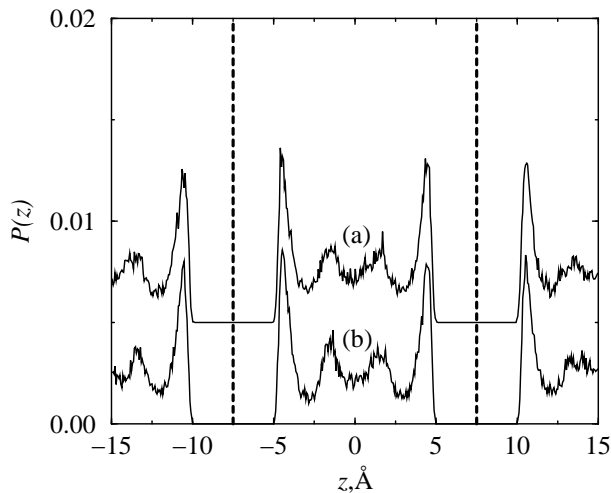


FIG. 7: Density profiles of water adsorption in graphene sheets at 550 K and reduced chemical potential of -26 . (a) was calculated using the atomistic summation potential and (b) was calculated using the integrated potential. Two curves are almost identical so (a) was shifted by 0.005 in $P(z)$ for clarity. The dashed lines at $z = \pm 7.5$ Å represent the two graphene sheets in the system.

of adsorbed methane in graphenes calculated using the atomistic and integrated potentials are in excellent agreement. Note that the density profiles calculated from the two potentials are almost identical to each other, so that we have to present them by shifting one curve along the vertical axis by a constant value to have a clear view.

The results for water adsorption in singlet graphenes at 550 K are shown in Figs. 6 and 7. It is seen from the water adsorption isotherm that a continuous wetting transition occurs at about $\mu^* = -33.4$. The density profile peaks corresponding to the first adsorbed layers on the graphene sheets locate at $z = \pm 4.4$ and ± 10.6 Å. Slightly different from that of methane, the adsorbed phase of water forms two second layers between the first layers, at $z = \pm 1.5$ and ± 13.5 Å, due to the relatively smaller size of water molecule compared to methane. The isotherms and density profiles of water in graphene sheets calculated from the integrated and atomistic potentials are also in excellent agreement. This indicates that the integrated potentials for multipolar interactions are also excellent approximations to the atomistic approach.

We monitored the computational time required for the simulations using two different approaches. It is found that typically the computational time for the integrated potential is $< 1\%$ of that required for the atomistic summations.

V. CONCLUSIONS

A set of effective potentials were derived for calculating the Lennard-Jones, dipole-induced dipole, dipole-quadrupole, and quadrupole-quadrupole interactions between fluid molecules and a graphene sheet. The integrated potential functions depend only on the separation between a molecule and the graphene surface. They are mathematically simple and easy to use in either estimating the interaction between a single molecule and a graphene sheet or in large-scale molecular simulations. The potential energies calculated from the integrated potentials are in excellent agreement with the results calculated from direct atomistic summations, while the integrated ones are computationally negligible compared with their atomistic counterparts. Adsorption simulations of two representative gases in singlet graphene sheets were performed to further test the derived potential functions. The adsorption isotherms and density profiles calculated from the derived potentials and atomistic models are in excellent agreement, indicating that the derived potential can predict both the equilibrium and the structural properties of adsorbed phase with excellent accuracy. The potentials developed in this work provide a simple, accurate, and robust method for calculating the physical interaction of molecules and single graphene sheets.

Finally, we note that the self-consistency in the polarization of carbon atoms by a polar fluid molecule was neglected in the derivation. However, we believe that the effect is relatively small compared with the dispersion, induction, and dipole-quadrupole interactions. Also, by using an integrated potential, one assumes the graphene surface is smooth and the impact of the surface corrugation on the molecule-solid interaction is ignored.

Acknowledgments

The author thanks Peter T. Cummings for many insightful discussions. This research was conducted at the Center for Nanophase Materials Sciences, which is sponsored at Oak Ridge National Laboratory by the Division of Scientific User Facilities, U.S. Department of Energy. This research used resources of the National Energy Research Scientific Computing Center, which is supported by the Office of Science of the U.S. Department of Energy under Contract No. DE-AC02-05CH11231.

-
- [1] Geim, A. K.; Novoselov, K. S. *Nature Materials* **2007**, *6*, 183.
 [2] Lee, C.; Wei, X. D.; Kysar, J. W.; Hone, J. *Science* **2008**,

321, 385–388.

- [3] Ponomarenko, L. A.; Schedin, F.; Katsnelson, M. I.; Yang, R.; Hill, E. W.; Novoselov, K. S.; Geim, A. K.

- Science* **2008**, *320*, 356–358.
- [4] Wang, F.; Zhang, Y. B.; Tian, C. S.; Girit, C.; Zettl, A.; Crommie, M.; Shen, Y. R. *Science* **2008**, *320*, 206–209.
- [5] Li, X. L.; Wang, X. R.; Zhang, L.; Lee, S. W.; Dai, H. J. *Science* **2008**, *319*, 1229–1232.
- [6] Li, D.; Müller, M. B.; Gilje, S.; Kaner, R. B.; Wallace, G. G. *Nature Nanotechnology* **2008**, *3*, 101–105.
- [7] Ruoff, R. *Nature Nanotechnology* **2008**, *3*, 10–11.
- [8] Schedin, F.; Geim, A. K.; Morozov, S. V.; Hill, E. W.; Blake, P.; Katsnelson, M. I.; Novoselov, K. S. *Nature Materials* **2007**, *6*, 652–655.
- [9] Fasolino, A.; Los, J. H.; Katsnelson, M. I. *Nature Materials* **2007**, *6*, 858–861.
- [10] Dikin, D. A.; Stankovich, S.; Zimney, E. J.; Piner, R. D.; Dommett, G. H. B.; Evmenenko, G.; Nguyen, S. T.; Ruoff, R. S. *Nature* **2007**, *448*, 457–460.
- [11] Abanin, D. A.; Lee, P. A.; Levitov, L. S. *Phys. Rev. Lett.* **2006**, *96*, 176803.
- [12] Novoselov, K. S.; Geim, A. K.; Morozov, S. V.; Jiang, D.; Katsnelson, M. I.; Grigorieva, I. V.; Dubonos, S. V.; Firsov, A. A. *Nature* **2005**, *438*, 197–200.
- [13] Zhang, Y.; Zhang, Y. B.; Tan, Y. W.; Stormer, H. L.; Kim, P. *Nature* **2005**, *438*, 201–204.
- [14] Meyer, J. C.; Girit, C. O.; Crommie, M. F.; Zettl, A. *Nature* **2008**, *454*, 319–322.
- [15] Steele, W. A. *Surf. Sci.* **1973**, *36*, 317–352.
- [16] Zhao, X. C.; Johnson, J. K. *Molecular Simulation* **2005**, *31*, 1–10.
- [17] Maitland, G. C.; Rigby, M.; Smith, E. B.; Wakeham, W. A. *Intermolecular Forces*; Clarendon Press: Oxford, 1981.
- [18] Jiang, S. Y.; Gubbins, K. E.; Zollweg, J. A. *Mol. Phys.* **1993**, *80*, 103–116.
- [19] Berendsen, H. J. C.; Grigera, J. R.; Straatsma, T. P. *J. Phys. Chem.* **1987**, *91*, 6269.
- [20] Rowley, R. L. *Statistical Mechanics for Thermophysical Property Calculations*; Prentice Hall: Englewood Cliffs, NJ, 1994.
- [21] Miller, T. M.; Bederson, B. In *Atomic and molecular polarizabilities: A Review of recent advances*; Bates, D. R., Bederson, B., Eds.; Academic Press: London, 1977; Vol. 13, pp 1–55.
- [22] Whitehouse, D. B.; Buckingham, A. D. *J. Chem. Soc., Faraday Trans.* **1993**, *89*, 1909–1913.
- [23] Allen, M. P.; Tildesley, D. J. *Computer Simulation of Liquids*; Clarendon Press: Oxford, 1987.
- [24] Gatica, S. M.; Johnson, J. K.; Zhao, X. C.; Cole, M. W. *J. Phys. Chem. B* **2004**, *108*, 11704.
- [25] Zhao, X. C. *Phys. Rev. B* **2007**, *76*, 041402.
- [26] Zhao, X. C.; Kwon, S. J.; Vidic, R.; Borguet, E.; Johnson, J. K. *J. Chem. Phys.* **2002**, *117*, 7719–7731.